Appendix I: Experimental Details

Alignment of an optical correlator system is of crucial importance, particularly the correct positioning of the spatial filter. By means of an iris diaphram both the target objects and SLM were centred very accurately. After the initial setup procedure - which requires one to pass an unexpanded laser beam at constant heoght above the bench throughout the system - an iris diaphram was placed a few cm before the object plane. With the diaphram closed to a diameter of only 2mm or so, its position was adjusted so pass the beam unhindered, upon which it was fully opened and the optical components of the bench installed. In the simulations, the target objects were centred in the object plane. By closing down the diaphram just before this plane, an almost circular beam of light falls on the centre of the object plane - diffraction effects being almost insignificant in between the diaphram and object planes. This allows accurate positioning of the target object.

With the target removed, the transform lens is placed in the system. By a suitable combination of auxiliary lenses the CCD array camera is focussed onto the frequency plane, where a `cross' pattern is displayed in amplitude mode as shown in figure 9.1.
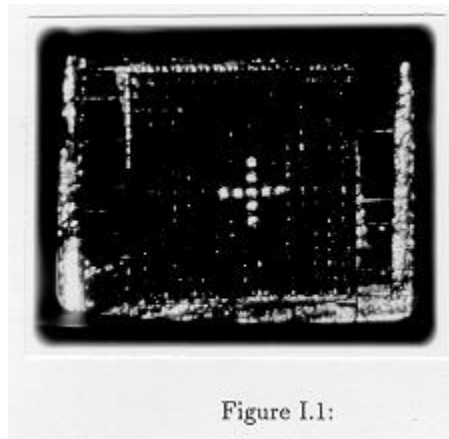

Figure I.1:

A polariser immediately after the laser is adjusted as required to reduce the intensity of the DC spot, the laser being used having a significant degree of polarisation. This pattern allows one to accurately centre the SLM in the frequency plane. The iris diaphram immediately before the object plane may again be closed down to 2mm or so and the circularly symmetric diffraction pattern should coincide with the centre of the displayed cross once the system has been correctly aligned.

Data Capture

The correlation images were captured with a 1024×1024 CCD array camera connected to an IBM PC using software developed by Will Hossack of the Applied Optics Group. Camera linearity has been checked within the Group [] and is in excess of 99.5%. Alongside the target object a small photoamplifier was placed to measure the slow time variations in laser intensity. The amplifier had previously been calibrated using a set of neutral density filters and found to provide an output voltage approximately linear with input light intensity over a large range. Suitable rotation of the polariser after the laser combined with translation of the photoamplifier away from the brighter (Gaussian) expaned beam enabled the device to measure laser beam fluctuations. At the instant a frame was `grabbed' the photoamplifier voltage was recorded.

The IBM data file was converted to DEC FORTRAN binary with the assistance of Will Hossack. A FORTRAN program was written to first search the captured file for the global maximum and, assuming this was a correlation peak, determine the best fitting Gaussian to the region surrounding the maximum. The coefficients of a cubic polynomial fitted to the photoamplifier graph of voltage vs light intensity, together with the voltage reading at the time the data was captured, enabled the file to be corrected for the laser beam fluctuations. These were, in fact, small but the correction allows scientific comparison between data captured at different times. Among the many other parameters determined were total image energy, percentage peak to total energy, offset of the peak from the file centre etc. of which a greatly reduced set have been incorporated in this thesis as useful figures of merit.

Figure 9.2 shows the effect of the image thresholding operation performed in chapter 8 on the auto-correlation results. This operation does little more than counter the contrast reducing effects observed to occur during the hardcopy process.
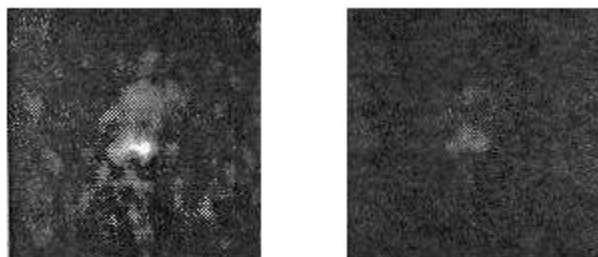

Figure I.2: Auto–correlation of letter 'C' with and without thresholding.

Figure I.2: Auto-correlation of letter `C' with and without thresholding.

Figure 9.3 illustrates the Gaussian fitting procedure described in chapter 7 so that the reader may appreciate the accuracy of the Gaussian parameter σ in quantitative analysis of the auto-correlations performed in chapter8.
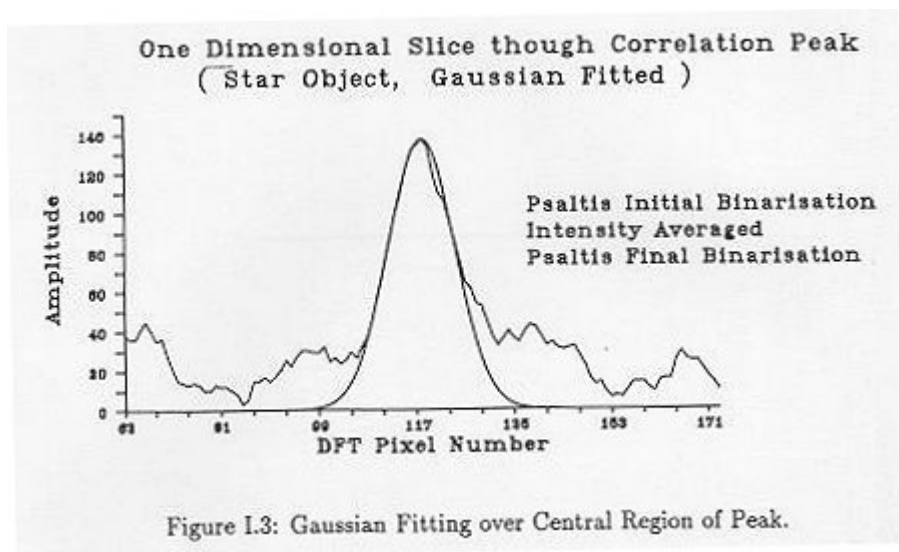

Figure I.3: Gaussian Fitting over Central Region of Peak.

Figure I.3: Gaussian Fitting over Central Region of Peak.